

Towards Distortion-tolerant Radio-interferometric Object Tracking

Gergely Zachár and Gyula Simon

Department of Computer Science and Systems Technology, University of Pannonia, Veszprém, Hungary

Keywords: Sensor Network, Localization, Tracking, Radio-interferometry, Phase Distortion, Fault Tolerance.

Abstract: Recently radio-interferometric object tracking methods were proposed, which apply inexpensive radio transmitter and receiver nodes to generate and measure radio-interferometric signals. The measured phase values can be used to track the position of one or more moving receivers. In these methods the ideal phase values, calculated from the position of the nodes, are heavily used. Unfortunately, multipath effects in indoor environments can significantly distort the ideal phase values, thus the accuracy and robustness of the former radio-interferometric methods is challenged. In this paper a novel position estimation method is proposed, which is less sensitive and thus more robust to distortions of radio-interferometric space. The performance of the proposed algorithm is compared to that of earlier radio-interferometric object tracking methods using simulations and real measurements.

1 INTRODUCTION

Recently several radio-interferometric (RI) object tracking methods were proposed (Zachár, 2014), (Zachár and Simon, 2015). These methods utilize inexpensive WSN nodes to generate the interferometric signals, and similar nodes to measure the relative phase values in various points in space. Some node positions are fixed and known, other nodes may move along unknown trajectories. From the measured phase values and the known node positions the unknown node positions can be calculated. These methods are especially useful indoors, where GPS signals are not available. The potential accuracy of the radio-interferometric methods is in the range of 10-20 centimeters, which make it an appealing solution where the performance of RSSI-based solutions (Au et al., 2012) is not satisfactory. Similar accuracy can be provided by RF time of flight ranging, but with more sophisticated hardware (Lanzisera et al., 2011), (Ye et al., 2011).

The formerly proposed RI tracking methods utilize ideal phase values, which are computed from the location of the nodes, assuming free signal propagation. In indoor environments, however, signal reflections, scattering, and diffraction (multipath effects) may heavily distort the ideal phase, thus the localization method use potentially imperfect data. The application of more precise propagation model in order to create more accurate phase map is practically

infeasible. The method proposed in this paper uses the potentially distorted phase maps but it is less sensitive to local distortions and thus it provides more robust tracking in indoor environments. The main contributions of the paper are the following:

- A new tracking method is proposed, which uses a confidence map calculated from unwrapped phase measurements and an unwrapped reference phase map;
- The novel tracking method is compared to earlier RI tracking solutions using simulations and real measurements.

The advantages of the proposed method are twofold:

- The algorithm provides more robust and more accurate estimates when the phase map is distorted due to multipath effects, which is a common situation indoors;
- The estimator has low computational complexity, thus it can be implemented in real time using conventional computers.

The outline of the paper is the following. In Section 2 related work is reviewed, including RI measurements and earlier tracking estimators. In Section 3 the new estimator is proposed. The performance of the proposed solution is analyzed in Section 4 through simulations and real measurements. Section 5 concludes the paper, including potential future work.

2 RELATED WORK

2.1 Interferometric Measurements

Radio interferometric measurements in the context of sensor networking were proposed by Maroti et al., (2005), where a Radio Interferometric Positioning System (RIPS) was created from low cost, of the shelf components. The radio-interferometric measurement process is illustrated in Figure 1, where two transmitters A and B generate the interference signal by transmitting carrier signals (sine waves) with almost the same frequency (f_A and f_B , respectively). The interference signal has low frequency envelope with frequency of $\Delta f = |f_A - f_B|$, measured by receivers C and D (the signal envelope is the RSSI signal itself). The phase difference ϑ of the measured RSSI signals depends on the relative positions of the quad A, B, C, and D, as follows:

$$\vartheta(\lambda) = 2\pi \frac{d_{ABCD}}{\lambda} \pmod{2\pi} \quad (1)$$

where

$$d_{ABCD} = d_{AD} - d_{BD} + d_{BC} - d_{AC} \quad (2)$$

with d_{AC} , d_{AD} , d_{BC} , and d_{BD} being pairwise distances shown in Figure 1, and λ is the wavelength of the carrier frequency ($\lambda \approx \lambda_A \approx \lambda_B$). Since the phase value ϑ is wrapped, i.e. $0 \leq \vartheta < 2\pi$, the exact value of d_{ABCD} cannot be determined, causing ambiguities in the solution. From multiple measurements using (a) different sets of measurement nodes, (b) different frequencies, or (c) both, the ambiguity can be resolved (Maroti et al., 2005). Unfortunately this solution requires high accuracy phase measurement, resulting long data collecting and processing times. Although the stochastic radio interferometric localization (SRIPS), proposed by Dil and Havinga (2011), can significantly reduce the required measurement and processing time, it still is not capable of tracking moving objects.

For object tracking, various approaches were proposed by Zachár et al., (2014a) and Zachár and Simon (2014b).

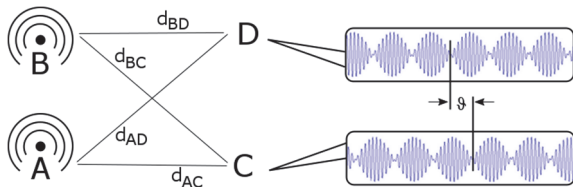


Figure 1: Radio interferometric measurements.

2.2 Interferometric Tracking

In interferometric tracking methods the position estimator is calculated using previous (known or estimated) positions, in addition to the interferometric measurements ϑ_n ($n = 1, 2, \dots, N$, where N is the number of quads providing measurements). Clearly, in tracking applications the initial node location must be known. Although with this approach the unknown location of an object cannot be determined without a priori information, but the main advantage is that this approach requires simple and fast measurements, using only one frequency, and allows much faster computations to estimate even the moving object's position in real time.

The tracking solutions utilize a fixed set of infrastructure nodes with known positions and one moving node, the position of which is to be tracked. Each measurement quad consists of three infrastructure nodes A, B, C, and the moving node D, according to Figure 1. Since three node locations are known, the unknown location of D can be calculated from (1), resulting a *set of hyperbolas* in two dimensions (Zachár et al., 2014a). Assuming that the sampling theorem is fulfilled (i.e. the measurements are frequent enough vs. the speed of the moving node), the tracking application proposed in (Zachár et al., 2014a) selects the hyperbola from the set of possible hyperbolas, which is closest to the hyperbola selected in the last time instant. This approach is equivalent to the expected continuity assumption, applied in general phase unwrapping problems (Tribolet, 1977).

Thus from the measurements of each quad a single hyperbola is derived, on which the moving object is located. The intersection of two such hyperbolas (determined from two quad measurements) provides a location estimate in two dimensions. In (Zachár and Simon, 2015a) the method was generalized to any number of hyperbolas, where instead of calculating potentially different intersections, a minimization problem was introduced, which contained squared distances from the calculated hyperbolas.

Instead of solving (1), i.e. calculating hyperbolas, a completely different approach was proposed for the location estimator in (Zachár and Simon, 2014b). Here the tracking is performed with the help of an error function $\varepsilon(p)$, defined as follows:

$$\varepsilon(p) = \frac{1}{N\pi^2} \sum_{n=1}^N (\Delta\vartheta_n(p))^2 \quad (3)$$

where p is an arbitrary position in the search space, N is the number of quad measurements, and $\Delta\vartheta_n$ is the

difference between the ideal $\vartheta_n^{(id)}$ and the measured ϑ_c phase difference values, as follows:

$$\Delta\vartheta_n(p) = \min_{i=-1,0,1} |\vartheta_n^{(id)}(p) + i2\pi - \vartheta_n| \quad (4)$$

The $\vartheta_n^{(id)}(p)$ values are calculated by applying (1) to the quad's node positions (notice that the infrastructure nodes' positions are known and the tracked node position is assumed to be p), while the ϑ_n values are measured. An example error map above a search space is shown in Figure 2(a). The error surface contains multiple minima (shown by red areas), among which one corresponds to the actual location (true minimum), the other are phantom minima. Again the expected continuity assumption is used and the solution is chosen as the local minimum closest to the estimated location in the previous time instant. An advantage of this approach is that the computational requirements of the error map are low, allowing real-time implementations without high hardware requirements.

The error map shown in Figure 2 is calculated from the ideal phase values of (1) and the measured phase differences, using (3). If the ideal phase values are different from the actual ones, e.g. because of multipath effects in the room, the error map becomes blurred, the local minima tend to 'melt' and merge. In such maps the solution is hard to find and potentially a wrong solution may be chosen. In the method of (Zachár and Simon, 2014b) the effect of choosing a wrong local minimum is critical: as the object moves, the phantom minimum, used as (erroneous) object position estimate, may disappear, thus a wrong choice results not only in estimation error but the object track can be lost. The algorithm in (Zachár and Simon, 2015b) enhances the performance of the algorithm when measurement errors are present, but does not handle the phase distortions problem.

In this paper a new estimator is proposed, which is not sensitive to phase distortions, thus the localization algorithm is more robust in indoors environments, where intense multipath effects can be expected.

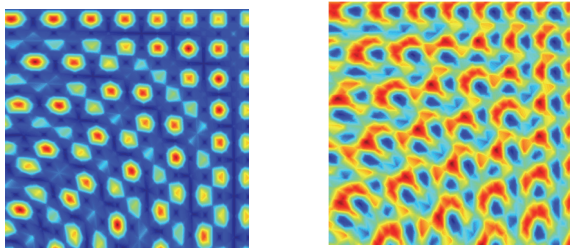


Figure 2: Error surfaces used in (Zachár and Simon, 2014b), (a) without phase distortion and (b) with phase distortion.

3 PROPOSED SOLUTION

3.1 Phase Distortion

The effect of phase distortion for the error map in (Zachár and Simon, 2014b) was illustrated in Figure 2. Now measurement results will be presented to validate the significance of the problem, and also to provide numerical data for the subsequent simulations.

Figure 3 shows phase difference measurement results, which were conducted in an office room. Two infrastructure transmitters A and B was used to generate the interferometric signal, and the phase difference was measured by the fixed infrastructure receiver C and the moving receiver D. Node D was moved along a linear trajectory on top of a table, and its position was recorded. The measured phase values, as a function of position of D, are shown in red in Figure 3. The ideal phase values, calculated using (1), are shown in blue. The measured phase values in general correspond well to the ideal values, but there are node areas where there is significant and systematic difference, e.g. between position 0.3m and 0.5m. These local distortions are the result of multipath effects, originating from RF propagation obstacles, e.g. the walls and furniture. The maximum discrepancy measured in the experiment was 0.19π .

3.2 Location Estimation

The error map of (3) utilizes the *wrapped* ideal phase values (1) and the *wrapped* measured phase values. The local distortion of the ideal phase values may cause significant distortion in the error surface. Thus a new error surface is proposed, constructed from unwrapped (ideal and measured) phase values.

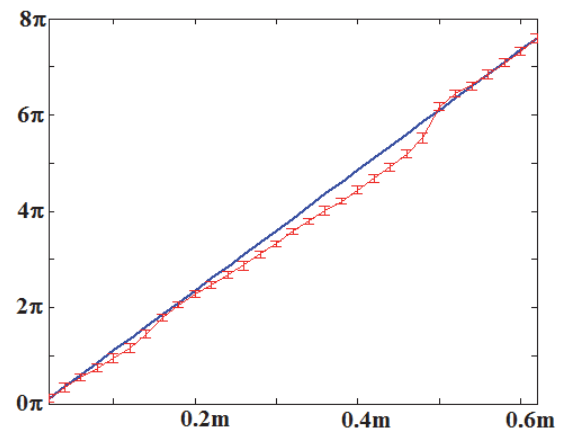


Figure 3: Measured (red) and ideal (blue) phase values, illustrating the phase distortion in indoor environment.

The ideal wrapped phase value at location p is $\vartheta_n^{(id)}(p)$, defined as follows:

$$\varphi_n^{(id)}(p) = 2\pi \frac{d_{ABCD}(p)}{\lambda} \quad (5)$$

where $d_{ABCD}(p)$ is calculated according to (2). Notice that (5) is the unwrapped version of (1). The distances d_{AC} , d_{AD} , d_{BC} , and d_{BD} in (2) are calculated from the known positions of nodes A, B, and C, while p is the position of node D.

Let us denote the (wrapped) phase values measured at time instant k by $\vartheta_n(k)$, $n = 1, 2, \dots, N$, where N is the number of quads utilized during the measurements. Since the tracked object is started from a known initial position p_0 at $k = 0$, the initial values for the measured phase values are set as follows:

$$\varphi_n(0) = \varphi_n^{(id)}(p_0) \quad (6)$$

For $k > 0$, the unwrapped measured phase values $\varphi_n(k)$ are calculated as follows:

$$\varphi_n(k) = \vartheta_n(k) + 2i\pi \quad (7)$$

where i is an integer s.t. $|\varphi_n(k) - \varphi_n(k-1)|$ is minimal (using the continuity assumption). An error surface is defined for each time instant k , as follows:

$$E(p, k) = \frac{1}{N} \sum_{n=1}^N \left(\varphi_n(k) - \varphi_n^{(id)}(p) \right)^2 \quad (8)$$

The location estimate at time instant k is the position p_{est} where $E(p, k)$ has its minimum:

$$p_{est}(k) = \underset{p}{\operatorname{argmin}} E(p, k) \quad (9)$$

3.3 Tracking Algorithm

The flowchart of the tracking algorithm is shown in Figure 4. In the initialization phase first the ideal phase maps are calculated for each quads (Step 1). The phase maps are calculated on a grid with resolution $\Delta p = 0.005\text{m}$. Notice that quads are formed from three infrastructure nodes and one tracked node such that the transmitter pairs A and B (chosen from the infrastructure nodes) are different in each quad. The choice of receiver node C is irrelevant, it can be any other infrastructure node, see e.g. (Zachár and Simon, 2015b). Thus in general, if K infrastructure nodes are deployed, maximum $N = \binom{K}{2}$ independent maps can be utilized.

When tracking is started at time instant zero, the known initial position p_0 is used to initialize the track

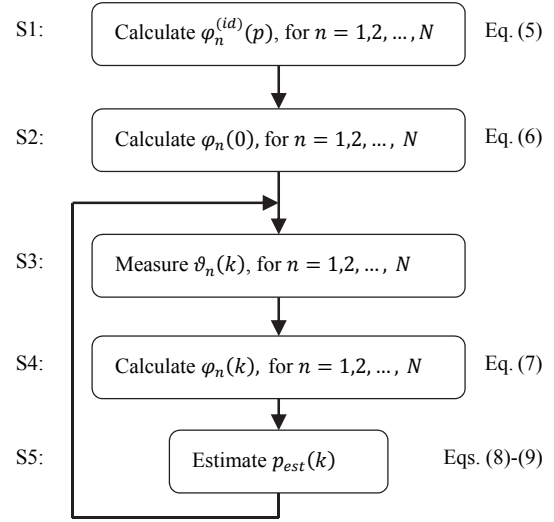


Figure 4: The flowchart of the tracking algorithm.

in Step 2. Then in each subsequent time instant a new measurement is performed in Step 3, to provide the wrapped phase measurements $\vartheta_n(k)$, $n = 1, 2, \dots, N$. Then the unwrapped measured phase values are calculated in Step 4, and the current position $p_{est}(k)$ is estimated in Step 5. The error map $E(p, k)$ in (8) is calculated above the same grid as the ideal maps in Step 1. Note that it is not necessary to calculate $E(p, k)$ for the whole grid; it is enough to make the calculation in the vicinity of $p_{est}(k-1)$. Steps 3-5 are repeated in each time instant.

The measurement process is repeated with a constant sampling interval Δt_{sampl} . In the current implementation, due to hardware limitations, $\Delta t_{sampl} = 42\text{ms}$. This sampling rate enables the tracking of objects with modest speed up to $v_{obj} = 2\text{m/s}$.

4 EVALUATION

To illustrate the efficiency of the proposed error surface, a simulation was performed to compare the effect of the phase distortion on the error surfaces of (Zachár and Simon, 2014b) and the proposed solution, and to compare the performance of the two localization algorithms. In the test a $4\text{m} \times 4\text{m}$ area was simulated, with four infrastructure nodes in the corners of the area. The fifth node to be tracked was moved along a circular trajectory, as shown in Figure 6.

From the four infrastructure nodes the transmitter pairs were chosen in six different ways, thus the tracking was performed by using six quads ($N = 6$).

The measurements were simulated in 200 node positions along the circle, according to (1), with $\lambda = 0.345\text{m}$ (corresponding to the ISM band at 868MHz). The measurements were corrupted with white measurement noise, using standard deviation of $\delta = 0.15\pi$. In addition to the noise, systematic distortion was also used to corrupt the measurements. The distortions were added to the measurements of two quads (out of six), with maximum amplitude of 0.2π , which corresponds well with measurement results of Figure 3. The simulations were conducted on a discrete grid, with a resolution of 0.01m.

The error surfaces of method (Zachár and Simon, 2014b) and the proposed method are shown in Figure 5. The peaks in Figure 5(a) are smeared, some of them are merged. The error surface of the proposed method has one significant global minimum, where the search is trivial.

The performances of the two methods are compared in Figure 6. The true trajectory, shown in red, is a full circle, starting from 6 o'clock position

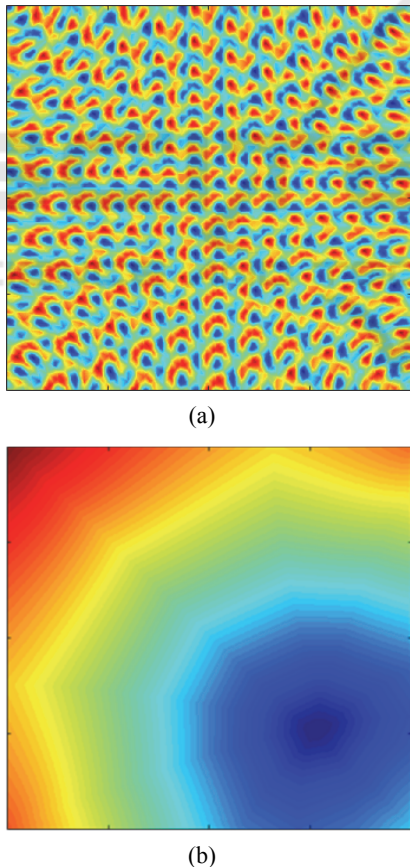


Figure 5: Error surfaces during the simulation test. (a) algorithm (Zachár and Simon, 2014b), (b) the proposed algorithm.

and going counter clockwise. Method (Zachár and Simon, 2014b) follows closely the true trajectory, when it disappears shortly after passing the 3 o'clock position, as shown in Figure 6(a). The proposed method was able to perform the tracking along the full trajectory, according to Figure 6(b). The maximum tracking error during the simulation was 0.09m, while the average error was 0.04m.

The performance of the proposed algorithm was tested with real measurements as well. The test hardware is described in (Zachár and Simon, 2015b). In the test four infrastructure nodes were used indoors, similarly to the simulation, placed at positions (0m, 0m), (9m, 0m), (9m, 6.1m), and (0m, 6.1m). In the experiment six quads were used ($N = 6$). The applied frequency was 868MHz, corresponding to $\lambda = 0.345\text{m}$. The phase values $\vartheta_n(k)$ were measured with $\Delta t_{\text{sampl}} = 42\text{ms}$. The fifth radio device to be tracked was moved along a circle with center of (4.5m, 3.05m) and radius of 1m, as shown in Figure 7 in red. The estimated positions, using the proposed algorithm, are shown in Figure 7 in blue. Notice the systematic error along several parts of the first half circle, probably because of phase

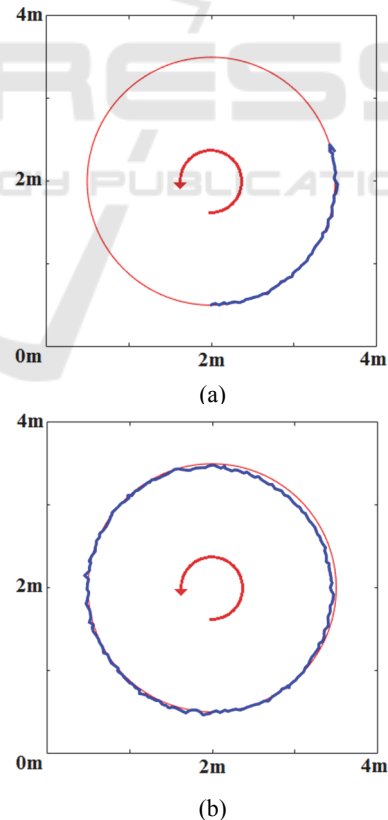


Figure 6: Simulated tracking results of (a) algorithm (Zachár and Simon, 2014b), (b) proposed method prediction.

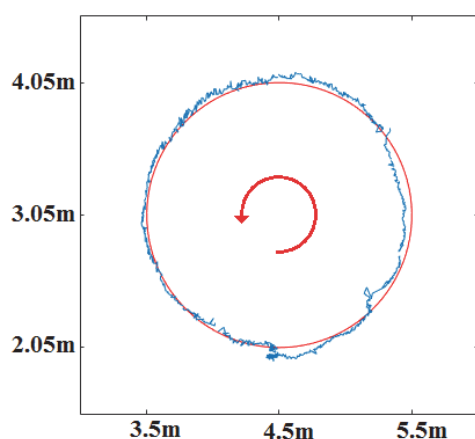


Figure 7: Real tracking results of the proposed algorithm. Red: ideal path, blue: estimated path.

distortions. Despite of this error, the method was able to track the object along the circle. The maximum tracking error during the experiment was 0.14m, while the average absolute error was 0.04m. The method of (Zachár and Simon, 2014b) lost track shortly after starting the circle (not shown in Figure 7).

The computation complexity of the proposed method is low: the calculation of the error map can be restricted to the neighborhood of the estimated previous position, thus the required time for the position estimation is constant in each round and independent of the measurement area. In the current implementation the evaluation of a measurement set takes less than 8ms in a 800x800 grid. Note that the required operations can be highly parallelized.

The proposed method highly outperforms RSSI-based methods, where the accuracy is in the range of meters (Au et al., 2013), and its accuracy is comparable to the best reported results of time of flight radio systems (Ye et al., 2011).

5 CONCLUSIONS

In this paper a novel object tracking method was proposed, which utilizes radio-interferometric phase measurements. The proposed solution enhances the robustness of the estimator and thus increases the accuracy of the position estimations when multipath effects, present in environment, cause distortions in the phase map, and thus the real phase map is different from the ideal one. The proposed method utilizes an error surface, created from the unwrapped ideal phase maps and the unwrapped measurement values. The proposed method shows more robust

behavior when phase distortions are present. The performance of the algorithm was illustrated by simulations and real measurements.

The proposed error-surface based algorithm is a significant step towards more robust radio-interferometric tracking: the potential problem of incorrect ideal phase map is correctly handled. The proposed method, however, requires unwrapped measured phase values, still presenting potential error sources: when the unwrapping is inaccurate (e.g. because of missing of faulty measurements) the position estimate may permanently remain biased. Future work includes self-correction mechanisms to provide tolerance against faulty measurements as well.

REFERENCES

- Au, A.W.S., et al, 2013. Indoor Tracking and Navigation Using Received Signal Strength and Compressive Sensing on a Mobile Device. *IEEE Transactions on Mobile Computing*, Vol. 12, No. 10, pp. 2050–2062.
- Dil B.J., Havinga, P.J.M., 2011. Stochastic Radio Interferometric Positioning in the 2.4 GHz Range. *Proceedings of the 9th ACM Conference on Embedded Networked Sensor Systems (SenSys 11)*, Seattle, WA, pp. 108-120.
- Lanzisera, S., Zats, D., Pister, K. S. J., 2011. Radio Frequency Time-of-Flight Distance Measurement for Low-Cost Wireless Sensor Localization. *IEEE Sensors Journal*, Vol. 11, No. 3, pp.837-845.
- Maroti M., et al, 2005. Radio Interferometric Geolocation. In *ACM Third International Conference on Embedded Networked Sensor Systems (SenSys 05)*, San Diego, CA, pp. 1-12.
- Tribolet, J.M. , 1977. A new phase unwrapping algorithm. *IEEE Transactions on Acoustics, Speech, and Signal Processing*, Vol. 25, No.2, pp. 170-177.
- Ye, T., Walsh, M., Haigh, P., Barton, J., O'Flynn, B., 2011. Experimental impulse radio IEEE 802.15.4a UWB based wireless sensor localization technology: Characterization, reliability and ranging. *22nd IET Irish Signals and Systems Conference ISSC 2011*, Dublin, Ireland, 23-24 Jun 2011.
- Zachár, G., Simon, G., Maróti, M., 2014a. Radio Interferometric Object Tracking. *Proc. 8th International Conference on Sensing Technology, ICST 2014*, pp. 453-458.
- Zachár, G., Simon, G., 2014b. Radio-Interferometric Object Trajectory Estimation. *Proc. 3rd International Conference on Sensor Networks, SENSORNETS 2014*, pp. 268-273.
- Zachár, G., Simon, G., 2015a. Radio Interferometric Tracking Using Redundant Phase Measurements. *Proc. 2015 IEEE International Instrumentation and Measurement Technology Conference, I2MTC 2015*, pp.2003-2008.
- Zachár, G., Simon, G., 2015b. Prediction-aided Radio-

interferometric Object Tracking. *Proc. 4th International Conference on Sensor Networks, SENSORNETS 2015*, pp. 161-168.

